MAJOR ARTICLE

Accelerated Detection of *Mycobacterium tuberculosis* Genes Essential for Bacterial Survival in Guinea Pigs, Compared with Mice

Sanjay K. Jain,[1,2,a] S. Moises Hernandez-Abanto,[1,a] Qi-Jian Cheng,[1] Prabhpreet Singh,[1] Lan H. Ly,[3] Lee G. Klinkenberg,[1] Norman E. Morrison,[1] Paul J. Converse,[1] Eric Nuermberger,[1] Jacques Grosset,[1] David N. McMurray,[3] Petros C. Karakousis,[1] Gyanu Lamichhane,[1] and William R. Bishai[1]

[1]Center for Tuberculosis Research and [2]Division of Pediatric Infectious Diseases, Johns Hopkins University School of Medicine, Baltimore, Maryland; [3]Department of Microbial and Molecular Pathogenesis, Texas A&M University System Health Science Center, College Station

Background. Mouse and guinea pig models have been used to identify *Mycobacterium tuberculosis* mutants attenuated for survival. However, unlike mice, *M. tuberculosis*–infected guinea pigs form caseating granulomas, which may simulate human disease more closely.

Methods. We used designer arrays for defined mutant analysis, a high-throughput subtractive competition assay, for genotypically defined *M. tuberculosis* mutants and compared the survival of the same mutant pools in guinea pig and mouse aerosol models. Selected mutants found to be attenuated in either aerosol model were also analyzed in the mouse hollow-fiber model.

Results. *M. tuberculosis* mutants representing 74 genes were tested. Eighteen *M. tuberculosis* mutants were attenuated for survival in either aerosol model, with 70% of selected mutants also attenuated in the mouse hollow-fiber model. The majority of attenuated mutants in the mouse aerosol model were detected only after 90 days of infection. There was a high degree of concordance between the genes identified by the 2 aerosol models, with detection being significantly earlier in the guinea pig ($P < .0003$).

Conclusions. We identified *M. tuberculosis* genes required for survival in mammalian lungs. The majority of mouse late-stage survival mutants were detected significantly earlier in the guinea pig, which suggests that differences in tuberculosis-induced lung pathologic changes may account for this accelerated detection.

Tuberculosis is one of the leading infectious causes of morbidity and mortality worldwide, with an estimated 8.8 million new patients acquiring tuberculosis each year [1]. Humans become infected with *Mycobacterium tuberculosis* via the respiratory route. After successful implantation, *M. tuberculosis* replicates in the lungs. This initial infection may lead to disease; however, it is frequently controlled by the host immune system, leading to latent infection. Identification of the *M. tuberculosis* genes required for survival in mammalian lungs may lead to the identification of key targets for drug and vaccine development [2].

Several defective growth phenotypes have been described by studying the in vivo growth patterns of *M. tuberculosis* mutants in mice [2, 3]. However, these phenotypes have not been characterized extensively in other animal models, particularly the ones that display caseous necrosis—the hallmark of the immune response to *M. tuberculosis* in humans. High-throughput techniques such as transposon (Tn) site hybridization have been developed, for the subtractive identification of attenuated Tn mutants, on the basis of microarray analysis [4, 5]. Recently, Lamichhane et al. [6] described designer arrays for defined mutant analysis (DeADMAn), a high-throughput, high-sensitivity approach for the subtractive identification of previously archived, genotypically defined *M. tuberculosis Himar1* Tn mutants attenuated for survival in mice after intravenous infection. In the present study, we used DeADMAn for the identification of

Received 2 November 2006; accepted 21 December 2006; electronically published 23 April 2007.

Potential conflicts of interest: none reported.

Financial support: National Institutes of Health (grants and contracts AI36973, AI43846, AI37856, and N01 AI30036).

[a] S.K.J. and S.M.H.-A. contributed equally to the study.

Reprints or correspondence: Dr. Sanjay K. Jain, Center for Tuberculosis Research, Johns Hopkins University School of Medicine, 1550 Orleans St., Baltimore, MD 21231 (sjain5@jhmi.edu).

The Journal of Infectious Diseases 2007; 195:1634–42

0022-1899/2007/19511-0012$15.00
DOI: 10.1086/517526

M. tuberculosis genes required for in vivo survival in mammalian lungs after aerosol infection. We also conducted a cross-species analysis by comparing the bacterial growth kinetics of identical pools of *M. tuberculosis* mutants in guinea pig and mouse aerosol models. Comparing species enabled a direct evaluation of the impact of caseous necrosis, which is present in guinea pig tuberculosis but absent in mouse tuberculosis [7].

MATERIALS AND METHODS

M. tuberculosis Himar1 *Tn mutants and media.* Random insertion mutagenesis of *M. tuberculosis* CDC 1551 strain was performed in our laboratory using the *Himar1* Tn as part of a comprehensive insertional mutagenesis study. Tn insertion sites were identified by sequencing the insertion junction as described elsewhere [8, 9]. Each mutant was grown separately at 37°C in Dubos broth base (Becton Dickinson) supplemented with Dubos medium albumin (Becton Dickinson), 5% glycerol, 0.01% sodium pyruvate, and 20 μg/mL kanamycin. All mutants used in the study, except for the positive and negative controls, were selected randomly. Two pools (A and B) containing 30 and 50 mutants, respectively, were prepared by combining a pure culture of each mutant grown to an OD_{600} of 0.8. Only mutants whose in vitro growth was similar to that of the wild type were used for the present study. Mutants that harbored a Tn in the region upstream of the terminal 100 bp (or, if the gene was <500 bp in length, within the 5′ 80% of the gene) were considered for screening, to decrease the likelihood of selecting distal mutations that might not disrupt gene-product function. In addition, 7 *M. tuberculosis* Tn mutants that harbored a Tn in the terminal 100 bp (or, if the gene was <500 bp in length, within the 3′ 20% of the gene) were also screened. *M. tuberculosis* Tn mutants JHU2583c-322 and JHU2675c-564 were included as positive and negative controls in each pool, respectively, because previous studies have shown that JHU2583c-322 (a Tn mutant in gene MT2660) is attenuated for survival in mice, whereas JHU2675c-564 (a Tn mutant in gene MT2749) is fully virulent [6]. Furthermore, *M. tuberculosis* Tn mutants JHU0842–1196 and JHU3833–375 (Tn mutants in genes MT0864 and MT3941, respectively) were present in both pools A and B. All mutants used in the study, including the controls, were subsequently found to have a Δ*sigF* background [10].

Guinea pig infection. Hartley strain guinea pigs weighing 250–300 g (Charles River Laboratories) were infected via the aerosol route using the latest version of the Madison Aerosol Chamber from the University of Wisconsin Engineering Shops [11]. Five guinea pigs per group were killed at days 1, 21, and 42 (pool A) and days 1, 21, 49, and 63 (pool B) after infection, and the survival of each mutant in the lungs was analyzed. Both lungs in their entirety were homogenized in PBS, and a significant proportion of the entire homogenate was plated on Middlebrook 7H10 solid medium (Becton Dickinson). For day 1 colony-forming unit counts, both lungs in their entirety were homogenized, and half of the homogenate was plated as above. Colony-forming unit counts were obtained by multiplying these results by a factor of 2. All plates were incubated at 37°C for at least 3 weeks before the colonies were counted or used for DNA preparation.

Mouse infection. Female BALB/c mice, 5–6 weeks old (Charles River Laboratories), were infected via the aerosol route using the Glas-Col inhalation exposure system (Glas-Col). Three mice per group were killed at days 1, 21, 49, 96, 147, and 360 after infection for both pools A and B, and the survival of each mutant in the lungs was analyzed. Both lungs in their entirety were homogenized in PBS and plated on Dubos broth base (Becton Dickinson) supplemented with Dubos medium albumin (Becton Dickinson), 1.5% agar, 5% glycerol, 0.01% sodium pyruvate, and 20 μg/mL kanamycin. For day 1 colony-forming unit counts, both lungs in their entirety were homogenized, and all of the homogenate was plated as described above. All plates were incubated at 37°C for at least 3 weeks before the colonies were counted or used for DNA preparation.

Microarray and real-time polymerase chain reaction (PCR) analysis. For each time point, the colonies from the plates were scraped and pooled, and genomic DNA was prepared using standard methods [12]. Two custom microarray sets (1 for each pool) were printed on poly-L-lysine–coated glass slides. Sixty-base oligonucleotides corresponding to the sequence at the junction of each Tn insertion were spotted 4 times in tandem on the microarray. The genomic DNA was digested with *Alu*I, the adapter was ligated, and junctions of Tn insertion sites were selectively PCR amplified using Tn-specific primers and were labeled with Cy3 and Cy5 monofluorescent dyes (Amersham Pharmacia) as described elsewhere [6]. Probes prepared from the input pool (1 day after infection) and output pools were cohybridized to custom microarrays and scanned by using a Genepix Axon 4000B device (Axon Instruments). Microarrays were performed at least in duplicate for each time point. The data were analyzed by use of a custom developed program [6]. Mutants with the input:output pool ratio significantly greater than or equal to the average of the negative and positive controls at a given time point were considered to be attenuated.

Real-time PCR analysis was performed to confirm and quantify the microarray results for mutants found to be attenuated by DeADMAn. Mutant-specific primer sets using Tn and gene-specific primers were designed to amplify 150–200-bp DNA fragments. These primer sets were tested using conventional PCR. All successful primer sets were used for mutant-specific real-time PCR using the iCycler IQ system (version 3.1.7050; Bio-Rad). The cycle threshold for genomic DNA from the input pool (1 day after infection) was compared with that from the output pool. For mutants not found to be attenuated at the

Table 1. *Mycobacterium tuberculosis* transposon (Tn) mutants ($n = 76$) tested in the guinea pig and mouse aerosol models.

JHU no.	MT no.	Rv no.	Function/probable function	Gene size, bp	Point of Tn insertion	Functional classification
JHU0031a-142	0031	…	Hypothetical protein	144	142	10
JHU0059-302	0065	0059	Hypothetical protein	693	302	16
JHU0346c-317	0361	0346c	L-asparagine permease, *ansP2*	1464	317	3
JHU0470c-98	0486	0470c	Mycolic acid synthase, *pcaA*	864	98	1
JHU0597c-1110	0627	0597c	Hypothetical protein	1236	1110	10
JHU0643c-815	0671	0643c	Methoxy mycolic acid synthase 3, *mmaA3*	906	815	1
JHU0755c-1269	0779	0755c	PPE family protein, *PPE12*	1941	1269	6
JHU0767c-209	0791	0767c	Hypothetical protein	642	209	10
JHU0842–1196	0864	0842	Integral membrane protein	1329	1196	3
JHU0892–43	0916	0892	Monooxygenase	1488	43	7
JHU0917-55	0942	0917	Glycine betaine transport integral membrane protein, *betP*	1782	55	3
JHU0989c-630	1018	0989c	Polyprenyl-diphosphate synthetase, *grcC2*	1002	630	7
JHU1013-512	1041	1013	Putative polyketide synthase, *pks16*	1614	512	1
JHU1021-27	1049	1021	Hypothetical protein	885	27	10
JHU1072-107	1102	1072	Transmembrane protein	837	107	3
JHU1115-208	1145	1115	Exported protein	699	208	3
JHU1127c-10	1159	1127c	Pyruvate phosphate dikinase, *ppdK*	1473	10	7
JHU1280c-1126	1317	1280c	Periplasmic oligopeptide-binding lipoprotein, *oppA*	1776	1126	3
JHU1376-857	1420	1376	Hypothetical protein	1494	857	10
JHU1545-152	1596.1	1545	Hypothetical protein	228	152	16
JHU1640c-1629	1678	1640c	Lysly-tRNA synthetase, *lysX*	3558	1629	2
JHU1660-514	1698	1660	Chalcone synthase, *pks10*	1062	514	10
JHU1682-732	1722	1682	Coiled-coil structural protein	849	732	10
JHU1742a-175	1742	…	Hypothetical protein	216	175	10
JHU1709-218	1750	1709	Hypothetical protein	837	218	10
JHU1757a-227	1757	…	Hypothetical protein	1161	227	10
JHU1808a-233	1808	…	Hypothetical protein	234	233	10
JHU1798-1340	1847	1798	Hypothetical protein	1833	1340	10
JHU1809-892	1857	1809	PPE family protein, *PPE33*	2085	892	6
JHU1876-63	1925	1876	Bacterioferritin, *bfrA*	480	63	7
JHU1901-590	1952	1901	cinA-like protein, *cinA*	1305	590	0
JHU1959c-13	2008	1959c	Hypothetical protein	297	13	10
JHU1992c-632	2048	1992c	Metal cation transporter P-type ATPase, *ctpG*	2316	632	3
JHU1994c-224	2050	1994c	Transcriptional regulatory protein	357	224	9
JHU2022c-605	2078	2022c	Hypothetical protein	606	605	10
JHU2059-599	2119	2059	Hypothetical protein	1536	599	10
JHU2114-561	2174	2114	Hypothetical protein	663	561	16
JHU2202c-74	2258	2202c	Carbohydrate kinase, *cbhK*	975	74	7
JHU2277c-441	2337	2277c	Glycerolphosphodiesterase	915	441	7
JHU2330c-241	2392	2330c	Lipoprotein, *lppP*	528	241	3
JHU2408-529	2481	2408	PE family protein, *PE24*	1005	529	6
JHU2413c-13	2486	2413c	Hypothetical protein	969	13	10
JHU2427c-331	2500	2427c	Gamma-glutamyl phosphate reductase, *proA*	1248	331	7
JHU2443-973	2519	2443	C4-dicarboxylate-transport transmembrane protein, *dctA*	1476	973	3
JHU2547-215	2623	2547	Hypothetical protein	273	215	10
JHU2657c-122	2734	2657c	phiRv2 phage protein	261	122	5
JHU2688c-201	2762	2688c	Antibiotic-transport ABC transporter	954	201	3
JHU2817c-248	2884	2817c	Hypothetical protein	1017	248	10
JHU2818c-1292	2885	2818c	Hypothetical protein	1293	1292	8

(continued)

Table 1. ***(Continued.)***

JHU no.	MT no.	Rv no.	Function/probable function	Gene size, bp	Point of Tn insertion	Functional classification
JHU2939-565	3009	2939	Polyketide synthase–associated protein, *papA5*	1269	565	1
JHU2950c-517	3023	2950c	Fatty-acid–CoA ligase, *fadD29*	1749	517	1
JHU3017c-20	3097	3017c	ESAT-6 like protein, *esxQ*	366	20	3
JHU3059-1148	3145	3059	Cytochrome P450, *cyp136*	1479	1148	7
JHU3062-1099	3148	3062	ATP-dependent DNA ligase, *ligB*	1524	1099	2
JHU3106-557	3189	3106	NADPH-ferredoxin reductase, *fprA*	1371	557	7
JHU3110-104	3193	3110	Pterin-4-alpha-carbinolamine dehydratase, *moaB1*	429	104	7
JHU3148-689	3236	3148	NADH dehydrogenase, chain B, *nuoD*	1197	689	7
JHU3428a-628	3428	…	Hypothetical protein	1146	628	10
JHU3447a-419	3447	…	PPE family protein	2288	419	6
JHU3352c-22	3460	3352c	Oxyreductase	372	22	7
JHU3490-976	3594	3490	Alpha, alpha-trehalose-phosphate synthase, *otsA*	1437	976	0
JHU3544c-320	3648	3544c	Acyl-CoA dehydrogenase, *fadE28*	1038	320	1
JHU3621c-463	3723	3621c	PPE family protein, *PPE65*	1242	463	6
JHU3622c-260	3724	3622c	PE family protein, *PE32*	300	260	6
JHU3639c-180	3741	3639c	Hypothetical protein	567	180	10
JHU3724B-154	3827	3724A	Cutinase precursor, *cut5A*	624	154	3
JHU3732-268	3837	3732	Hypothetical protein	1059	268	10
JHU3788-317	3896	3788	Hypothetical protein	486	317	16
JHU3831-293	3939	3831	Hypothetical protein	483	293	16
JHU3832c-450	3940	3832c	Hypothetical protein	588	450	10
JHU3833-375	3941	3833	Transcriptional regulatory protein	792	375	9
JHU3864-351	3978	3864	Hypothetical protein	1209	351	10
JHU3878-235	3992	3878	Hypothetical protein	843	235	16
JHU3900c-27	4017	3900c	Hypothetical protein	936	27	10
JHU2583c-322	2660	2583c	GTP pyrophosphokinase, *relA*			Positive control
JHU2675c-564	2749	Rv2675c	Hypothetical protein			Negative control

NOTE. Seven *M. tuberculosis* Tn mutants that harbor a Tn in the terminal 100 bp (or if the gene was <500 bp in length, within the 3′ 20% of the gene) and the positive and the negative control mutants are in bold type. Functional classification key [14]: 0, virulence; detoxification, and adaptation; 1, lipid metabolism; 2, information pathways; 3, cell wall and cell processes; 5, insertion sequences and phages; 6, PE/PPE; 7, intermediary metabolism and respiration; 8, unknown; 9, regulatory proteins; 10, conserved hypotheticals; 16, conserved hypotheticals with ortholog in *M. bovis*. CoA, coenzyme A; ESAT, early secreted antigen target; PE, proline-glutamic acid; PPE, proline-proline-glutamic acid.

time point indicated by microarray analysis, real-time PCR was performed at all subsequent time points available for that pool. Real-time PCR was performed at least in triplicate for each mutant.

Mouse hollow-fiber infection. Pool B culture containing 50 mutants was encapsulated into polyvinylidene fluoride hollow fibers and implanted subcutaneously into 6–8-week-old SKH1 hairless mice (Charles River Laboratories), as described elsewhere [13]. Four mice (each of which contained 2 hollow fibers) were killed at days 1 and 56 after infection. The hollow-fiber contents were recovered and plated on Middlebrook 7H10 solid medium (Becton Dickinson). For each time point, the colonies from the plates were scraped and pooled, and genomic DNA was prepared using standard methods [12]. Real-time PCR analysis was performed for all pool B mutants found to be attenuated for survival in the guinea pig and mouse aerosol models. The cycle threshold for genomic DNA from the input pool (1 day after infection) was compared with that from the output pool (56 days after infection). Real-time PCR was performed at least in triplicate for each mutant.

Statistical analysis. Kaplan-Meier survival curve analysis was done using Prism 4 software (version 4.01; GraphPad Software).

RESULTS

M. tuberculosis *Tn mutants tested and attenuated for survival in the guinea pig and mouse aerosol models.* A total of 80 *M. tuberculosis* Tn mutants were used to infect both the guinea pig and mouse via the aerosol route (table 1). After aerosol infection, day 1 $\log_{10}$ colony-forming units were 3.48 ± 0.06 and 3.40 ± 0.28 for pools A and B, respectively, for mouse lungs and 2.07 ± 0.17 and 2.29 ± 0.07 for pools A and B, respectively, for guinea pig lungs.

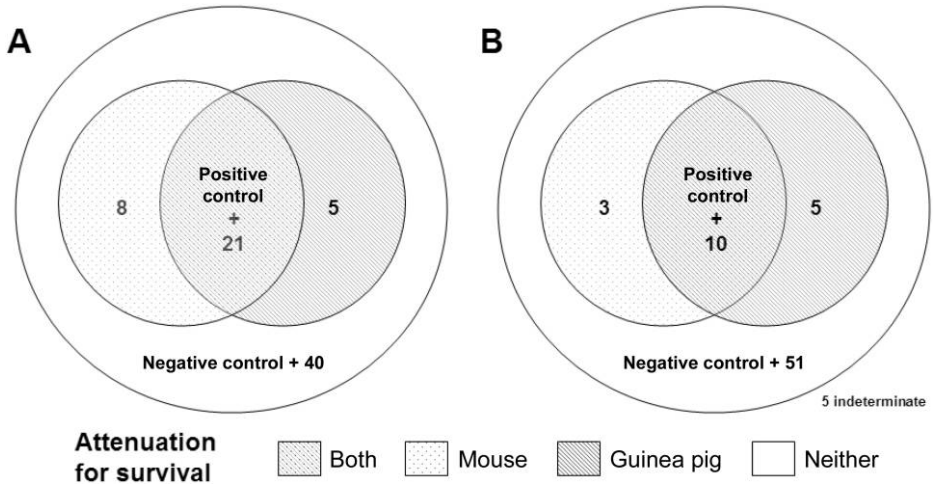

Figure 1. Results after microarray and real-time polymerase chain reaction (PCR) analysis. *A,* Thirty-four *Mycobacterium tuberculosis* transposon (Tn) mutants, attenuated for survival in either the guinea pig or mouse aerosol models after microarray analysis. There was a high degree of agreement between the mutants found to be attenuated for survival in guinea pig lung, compared with mouse lung (κ coefficient, 0.63; agreement, 0.83). *B,* Eighteen *M. tuberculosis* Tn mutants, attenuated for survival in either the guinea pig or mouse aerosol models after real-time PCR analysis. Again, there was a high degree of agreement between the mutants found to be attenuated for survival in guinea pig lung, compared with mouse lung (κ coefficient, 0.64; agreement, 0.89). JHU2583c-322 (positive control), JHU2675c-564 (negative control), JHU0842-1196, and JHU3833-375 were present in both pools A and B and yielded the same results in both pools and both models.

DeADMAn screening on day 1 (input pool) confirmed the lung implantation of each mutant in both pools and models used. As expected, the positive and negative controls were found to be attenuated for survival and fully virulent, respectively, in both pools and models. Similarly, *M. tuberculosis* Tn mutants JHU0842-1196 and JHU3833-375 were found to yield similar results in both pools and models. Thirty-four *M. tuberculosis* Tn mutants were found to be attenuated for survival in either the guinea pig or mouse lung. Of these, 26 were found to be attenuated for survival in the guinea pig model, whereas 29 were attenuated in the mouse model (figure 1*A*). There was a high degree of agreement between the mutants found to be attenuated for survival in the guinea pig lung, compared with mouse lung (κ coefficient, 0.63; agreement, 0.83). To confirm and quantify the DeADMAn results, real-time PCR was performed for the 34 *M. tuberculosis* Tn mutants attenuated for survival. Primer sets for 5 mutants (JHU1021-27, JHU1127c-10, JHU2202c-74, JHU3447a-419, and JHU3352c-22) were unsuccessful in amplifying a specific PCR product and were removed from further analysis. Eighteen mutants were found to be attenuated for survival in either the guinea pig or mouse aerosol models. Of these, 15 were found to be attenuated for survival in the guinea pig, whereas 13 were attenuated in the mouse (table 2). Again, there was a high degree of agreement between the mutants found to be attenuated for survival in the guinea pig lung, compared with mouse lung (κ coefficient, 0.64; agreement, 0.89), which suggests a high degree of concordance for *M. tuberculosis* genetic requirements for growth between the 2 models (figure 1*B*).

Mutants for 9 of 13 genes attenuated for survival in the mouse were detected only after 90 days of infection. Furthermore, as expected, 6 of 7 Tn mutants with Tn insertions in the distal portion of the genes were not found to be attenuated in either the guinea pig or mouse aerosol models. However, mutant JHU1742a-175 was found to be attenuated in both the guinea pig and mouse models. This mutant harbors the Tn insertion just distal (80.5%) to the 80% cutoff used in the study, and it is therefore likely that the Tn insertion was successful in inactivating this gene.

Mouse hollow-fiber infection. As proof of principle, selected mutants found to be attenuated for survival in either the guinea pig or mouse aerosol models were also analyzed using real-time PCR in the mouse hollow-fiber model [13]. In this novel in vivo model, granulomatous lesions develop around encapsulated bacilli in semidiffusible hollow fibers implanted subcutaneously into mice. In this microenvironment, the organisms demonstrated an altered physiologic state characterized by stationary-state colony-forming unit counts and decreased metabolic activity. Seven of 10 mutants tested in this model were found to be attenuated by day 56 after infection (table 2), which suggests that these genes may be important for the extracellular survival of *M. tuberculosis* within granulomatous lesions.

Functional classification of genes represented by the* M. tuberculosis *Tn mutants. Table 3 summarizes the functional classification of genes represented by the *M. tuberculosis* Tn mutants. Mutants in 74 unique genes spanning 11 *M. tuberculosis* genetic functional classes were tested [14, 15]. Forty-one

Table 2. *Mycobacterium tuberculosis* transposon (Tn) mutants found to be attenuated for survival in the guinea pig and mouse aerosol models.

MT no.	Rv no.	Function/probable function	Functional classification	Survival attenuation detected (fold attenuation), days after infection		
				Guinea pigs	Mice	Hollow fiber
0361	0346c	L-asparagine permease, *ansP2*	3	42 (9.2 ± 5.7)	360 (3.5 ± 1.5)	…
0864	0842	Integral membrane protein	3	63 (41.3 ± 3.1)	49 (3.4 ± 2.4)	56 (2.9 ± 1.1)
1102	1072	Transmembrane protein	3	49 (9.4 ± 5.8)	360 (14.6 ± 1.1)	NA[a]
1698	1660	Chalcone synthase, *pks10*	2	NA[b]	360 (2.4 ± 1.2)	…
1742	…	Hypothetical protein	10	49 (7.1 ± 6.0)	NA[c]	NA[a]
1750	1709	Hypothetical protein	10	NA[b]	49 (3.1 ± 1.9)	…
1847	1798	Hypothetical protein	10	49 (20.2 ± 7.4)	21 (10.8 ± 1.3)	56 (7.0 ± 3.5)
2048	1992c	Metal cation transporter P-type ATPase, *ctpG*	3	42 (4.4 ± 2.5)	NA[c]	…
2050	1994c	Transcriptional regulatory protein	9	42 (58.4 ± 1.8)	360 (39.4 ± 2.0)	…
2174	2114	Hypothetical protein	16	NA[d]	360 (10.3 ± 1.5)	56 (1.7 ± 1.2)
2500	2427c	Gamma-glutamyl phosphate reductase, *proA*	7	63 (4.3 ± 1.4)	360 (8.6 ± 2.5)	56 (3.4 ± 1.2)
2884	2817c	Hypothetical protein	10	49 (2.9 ± 1.7)	360 (3.1 ± 2.1)	NA[a]
3097	3017c	ESAT-6–like protein, *esxQ*	3	42 (38.5 ± 1.1)	360 (58.4 ± 4.8)	…
3236	3148	NADH dehydrogenase, chain B, *nuoD*	7	42 (1702.4 ± 4.6)	NA[c]	…
3594	3490	Alpha, alpha-trehalose phosphate synthase, *otsA*	0	21 (194.0 ± 7.4)	NA[c]	56 (5.0 ± 1.1)
3648	3544c	Acyl-CoA dehydrogenase, *fadE28*	1	42 (4.0 ± 1.1)	49 (13.9 ± 2.0)	…
3827	3724A	Serine esterase, cutinase family, *cut5A*	7	49 (3.6 ± 1.8)	NA[c]	56 (2.6 ± 1.3)
3978	3864	Hypothetical protein	10	49 (3.2 ± 1.7)	360 (7.8 ± 1.3)	56 (2.0 ± 1.2)

NOTE. Eighteen *M. tuberculosis* Tn mutants were found to be attenuated for survival in either the guinea pig or the mouse aerosol model. Fifteen were found to be attenuated for survival in the guinea pig model, and 13 were attenuated in the mouse model, with a high degree of agreement between the 2 models. Of these, 7 of 10 mutants tested in the hollow-fiber model were also found to be attenuated for survival. Genes in bold type are late-stage survival genes detected only after 90 days of infection in the mouse lung. Fold attenuation is the mean ± SD. Functional classification key [14]: 0, virulence, detoxification, and adaptation; 1, lipid metabolism; 2, information pathways; 3, cell wall and cell processes; 7, intermediary metabolism and respiration; 9, regulatory proteins; 10, conserved hypotheticals; 16, conserved hypotheticals with an ortholog in *M. bovis*. CoA, coenzyme A; ESAT, early secreted antigen target; NA, not attenuated.

[a] Up to day 56.
[b] Up to day 42.
[c] Up to day 360.
[d] Up to day 63.

percent were conserved hypotheticals, 16% were involved with cell wall/cell processes, 16% were involved with intermediary metabolism/respiration, and the remaining 27% distributed among other functional classes. Forty-two percent (5/12) of genes involved with cell wall/cell processes, 25% (3/12) of the genes involved with intermediary metabolism/respiration, and 20% (6/30) of conserved hypotheticals were found to be attenuated for survival. Thirty-three percent (3/9) of the genes identified for late-stage survival (after 90 days) in the mouse lung were involved with cell wall/cell processes.

Time to detection of attenuation for the survival of* M. tuberculosis *Tn mutants. Of the 13 *M. tuberculosis* Tn mutants found to be attenuated in the mouse aerosol model, less than one-third (4/13) were detected by day 49. We hypothesized that the guinea pig aerosol model would be immunologically different from the mouse model because of the presence of caseous necrosis [7]. Indeed, 87% (13/15) of Tn mutants found to be attenuated in the guinea pig aerosol model were detected by day 49. Figure 2 shows the comparison of Kaplan-Meier survival curves for the attenuated Tn mutants. Median survival times of Tn mutants in guinea pig and mouse aerosol models were 49 and 360 days, respectively ($P < .0001$, log-rank test). When this comparison was made for the 10 Tn mutants attenuated in both the guinea pig and mouse aerosol models, median mutant survival times were still significantly shorter in the guinea pig ($P = .0003$, log-rank test). These data show that the guinea pig model detects attenuation for the survival of *M. tuberculosis* mutants earlier than the mouse model.

DISCUSSION

M. tuberculosis is an extensively host-adapted pathogen that has developed strategies to survive intracellularly (in macrophages and nonprofessional phagocytic cells), disseminate outside of the lungs, and resist both innate and adaptive immune mechanisms, the latter of which is required in humans for the development of caseating granulomas. At least 4 classes of *M. tuberculosis* survival defects have been described through the study of *M. tuberculosis* mutants in mice; these include defective growth in vivo attenuation (giv), severe growth in vivo (sgiv),

Table 3. Functional classification of the genes represented by the *Mycobacterium tuberculosis* transposon (Tn) mutants.

Functional classification [14]	*M. tuberculosis* Tn mutants, no. Tested	Attenuated for survival
Virulence, detoxification, and adaptation	2	1
Lipid metabolism	6	1
Information pathways	2	1
Cell wall and cell processes	12	5
Insertion sequences and phages	1	0
PE/PPE family	6	0
Intermediary metabolism and respiration	12	3
Unknown	1	0
Regulatory proteins	2	1
Conserved hypotheticals	24	5
Conserved hypotheticals with and ortholog in *M. bovis*	6	1

NOTE. Mutants in 74 unique genes spanning 11 *M. tuberculosis* genetic functional classes were tested. A total of 41% were conserved hypotheticals, 16% were involved with cell wall/cell processes, 16% were involved with intermediary metabolism/respiration, and the remaining 27% were distributed among other functional classes. Forty-two percent (5/12) of genes involved with cell wall/processes, 25% (3/12) of genes involved with intermediary metabolism/respiration, and 20% (6/30) of conserved hypotheticals were found to be attenuated for survival. PE, proline-glutamic acid; PPE, proline-proline-glutamic acid.

persistence (per), and pathology (pat) or immunopathology (imp) phenotypes [2, 16]. However, mutants displaying these phenotypes have not been extensively characterized in animal models, such as the guinea pig, that form caseating necrosis as part of their adaptive immune response to *M. tuberculosis*. Previous studies have shown that the *M. tuberculosis* Δ*sigC* mutant was found to have a giv phenotype in guinea pigs [17] but an imp phenotype in mice [18]. Recently, Converse et al. have shown that the *M. tuberculosis* Δ*dosR* mutant has a giv phenotype in guinea pigs. In mice, however, this same mutant has a giv phenotype at 4–8 weeks but no significant growth defect by 6 months after infection (P. J. Converse, P. C. Karakousis, S. S. Allen, et al., unpublished data). These data suggest different bacterial survival kinetics for *M. tuberculosis* mutants in guinea pig and mouse models. Therefore, in the present study, we compared the kinetics of bacterial survival in mammalian lungs of identical pools of *M. tuberculosis* mutants in 2 aerosol models, to directly evaluate the impact of caseous necrosis seen in guinea pig tuberculosis [7] but not in mouse tuberculosis. Furthermore, mutants for select genes required for survival in mammalian lungs were also evaluated in the hollow-fiber dormancy mouse granuloma model.

DeADMAn is a high-throughput, subtractive identification screening tool for the competitive survival of defined mutant pools. This approach has been shown to be highly sensitive for up to 100 mutants/pool [6]. In the present study, we used smaller pools of up to 50 mutants, because only a limited number of bacilli can be implanted in the lungs by the aerosol route. It should be noted that DeADMAn uses pooled mutant infections, which may confound results because of complementation of defective mutants by extracellular factors secreted by other mutants in the same pool. Furthermore, because DeADMAn is an indirect measure of colony-forming units, it is not useful for the identification of imp/pat mutants. All mutants used in the present study have a Δ*sigF* background [10]. However, because mutants were normalized against controls with the same Δ*sigF* background, a Tn-disrupted gene rather than a *sigF* deletion is likely responsible for the observed phenotype. Nonetheless, potential interaction of the *sigF* deletion with the Tn-disrupted gene cannot be completely ruled out. Finally, the *M. tuberculosis* CDC 1551 strain was used in the study, and certain animal models have shown that this strain is less virulent than the H37Rv strain [19]. However, we believe that these 2 strains are highly comparable. Furthermore, because comparisons were made against controls with the same background, the Tn-disrupted gene rather than the background strain is responsible for the observed phenotype. Nonetheless, it is possible that a similar analysis in the H37Rv background may result in a somewhat different list of mutants attenuated for survival than found in the present study.

Eighteen *M. tuberculosis* genes were identified in the present study to be required for survival in mammalian lungs. These include MT1847 (Rv1798) and MT3648 (Rv3544c), which have been previously described for in vivo survival in mouse lungs and spleens, respectively [5, 6], and MT3594 (*otsA,* Rv3490), whose deletion mutant has been shown to be attenuated in

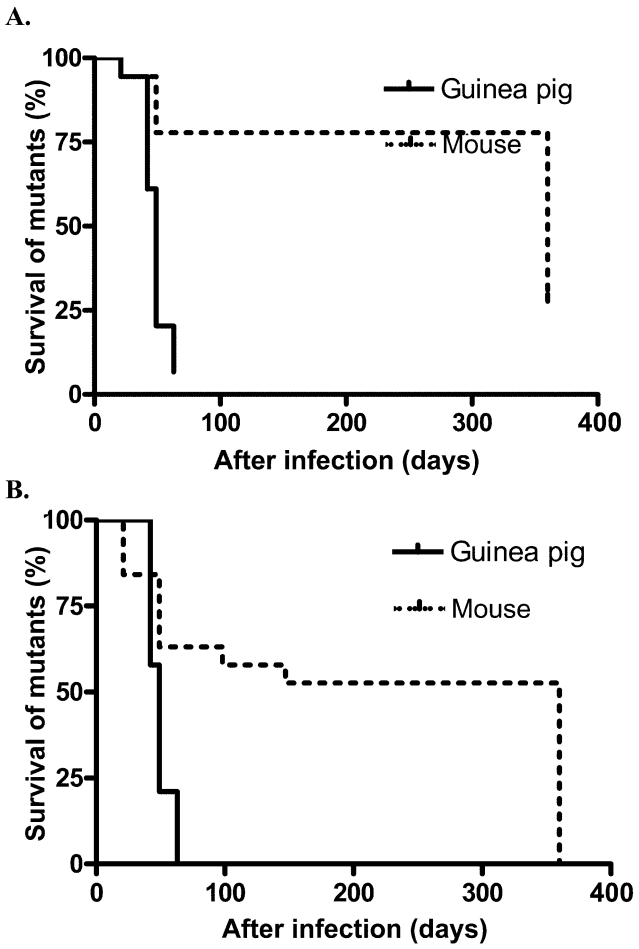

Figure 2. Kaplan-Meier survival comparison for attenuated mutants. *A,* Survival-curve analysis for 18 *Mycobacterium tuberculosis* transposon (Tn) mutants attenuated either in the guinea pig or mouse aerosol model. Median survival times of Tn mutants in the guinea pig model were significantly shorter than those in the mouse model ($P < .0001$, log-rank test). *B,* Survival-curve analysis for 10 *M. tuberculosis* Tn mutants attenuated in both the guinea pig and mouse models. Median survival times of Tn mutants in the guinea pig model were significantly less than those in the mouse model ($P = .0003$, log-rank test). These data show that the guinea pig model detects attenuation for survival earlier than the mouse aerosol model.

mouse lung and spleen after intravenous infection [20]. MT1847 (Rv1798), MT3236 (*nuoD,* Rv3148), and MT3594 (*otsA,* Rv3490) have been found to be up-regulated during nutrient starvation, which suggests their role in mycobacterial responses to the host environment [21]. Of the genes identified in the present study, 9 were required for in vivo survival in the mouse lung for >90 days. We believe that these genes are required for late-stage survival and represent key virulence factors required for survival in maturing granulomatous lesions. These late-stage survival genes include MT1102 (Rv1072) and MT2050 (Rv1994c), which have been found to be up-regulated during nutrient starvation and oxidative stress [21, 22]. MT1102 (Rv1072) and MT2050 (Rv1994c) are both SigH-dependent genes [16, 23], which suggests their role in adaptive responses to the host immune system. Similarly, MT0361 (Rv0346c) and MT2174 (Rv2114) were found to be up-regulated under different stress conditions, including the anaerobic/micro-aerophilic environment [24] and nutrient starvation [21], which suggests their possible role in survival against the host immune response. MT1698 (*pks10*, Rv1660) is required for phthiocerol dimycocerosate synthesis, and mutants deficient in this gene are attenuated for survival in the mouse lung [25]. In addition, it is also up-regulated during nutrient starvation [21]. MT3978 (Rv3864) has been previously described to be required for in vivo survival in the mouse spleen [5] and has also been found to be up-regulated during nutrient starvation [21]. Further studies are under way to validate our screen and to characterize these mutants to better understand their function(s).

Unlike mice, *M. tuberculosis* disease in guinea pigs leads to well-formed caseous granulomas [7]. It was therefore hypothesized that mouse late-stage survival mutants might lack key virulence pathways required for survival in maturing granulomatous lesions and that the presence of caseous necrosis in guinea pig granulomas might accelerate their detection. In other words, well-formed granulomas in guinea pigs might impose more intense, albeit similar, stressors, compared with the poorly formed granulomas observed in mice, and lead to accelerated detection of these late-stage survival mutants. Indeed, as hypothesized, the guinea pig model was found to detect attenuation for survival of the majority of the Tn mutants earlier than the mouse lung model. Furthermore, 10 mutants required for survival in mammalian lungs were evaluated in the hollow-fiber mouse granuloma model, and 7 were found to be attenuated for survival in this model, which suggests that the genes represented by those mutants are important for *M. tuberculosis* survival within granulomatous lesions. Our hypothesis is further strengthened by the fact that several of the genes detected earliest in the guinea pig model, compared with the mouse model (MT0361 [Rv0346c], MT1102 [Rv1072], MT2050 [Rv1994c], and MT3978 [Rv3864]), are likely to be involved with responses to stressors generated by the host immune response, such as granulomas [16, 21–24].

In summary, using a competition survival assay, we have identified genes required for bacterial survival in mammalian lungs after aerosol infection. There was a high degree of agreement between the genes identified by each of the models used. Long-term mouse infection showed that certain late-stage survival bacterial mutants survived for >90 days but later were out-competed by other mutants in the pools between days 150 and 360. Majority of these mouse late-stage survival mutants were identified in <65 days in the guinea pig model. Mouse late-stage survival mutants may lack key virulence pathways required for survival in maturing granulomatous lesions, and

the presence of caseous necrosis in guinea pig granulomas may accelerate their detection. Further studies are under way to characterize these mutants and to better understand their function(s) in well-formed granulomas.

Acknowledgment

We appreciate the assistance of Nacer Lounis in the study.

References

1. World Health Organization. Global tuberculosis control—surveillance, planning, financing. Available at: http://www.who.int/tb/publications/global_report/en/. Accessed 1 November 2006.
2. Hingley-Wilson SM, Sambandamurthy VK, Jacobs WR Jr. Survival perspectives from the world's most successful pathogen, *Mycobacterium tuberculosis.* Nat Immunol **2003**; 4:949–55.
3. Nuermberger E, Bishai WR, Grosset JH. Latent tuberculosis infection. Semin Respir Crit Care Med **2004**; 25:317–36.
4. Sassetti CM, Boyd DH, Rubin EJ. Genes required for mycobacterial growth defined by high density mutagenesis. Mol Microbiol **2003**; 48: 77–84.
5. Sassetti CM, Rubin EJ. Genetic requirements for mycobacterial survival during infection. Proc Natl Acad Sci USA **2003**; 100:12989–94.
6. Lamichhane G, Tyagi S, Bishai WR. Designer arrays for defined mutant analysis to detect genes essential for survival of *Mycobacterium tuberculosis* in mouse lungs. Infect Immun **2005**; 73:2533–40.
7. Turner OC, Basaraba RJ, Orme IM. Immunopathogenesis of pulmonary granulomas in the guinea pig after infection with *Mycobacterium tuberculosis.* Infect Immun **2003**; 71:864–71.
8. Lamichhane G, Zignol M, Blades NJ, et al. A postgenomic method for predicting essential genes at subsaturation levels of mutagenesis: application to *Mycobacterium tuberculosis.* Proc Natl Acad Sci USA **2003**; 100:7213–8.
9. Rubin EJ, Akerley BJ, Novik VN, Lampe DJ, Husson RN, Mekalanos JJ. In vivo transposition of mariner-based elements in enteric bacteria and mycobacteria. Proc Natl Acad Sci USA **1999**; 96:1645–50.
10. Chen P, Ruiz RE, Li Q, Silver RF, Bishai WR. Construction and characterization of a *Mycobacterium tuberculosis* mutant lacking the alternate sigma factor gene, *sigF.* Infect Immun **2000**; 68:5575–80.
11. Wiegeshaus EH, McMurray DN, Grover AA, Harding GE, Smith DW. Host-parasite relationships in experimental airborne tuberculosis. 3. Relevance of microbial enumeration to acquired resistance in guinea pigs. Am Rev Respir Dis **1970**; 102:422–9.
12. Larsen M. Some common methods in mycobacterial genetics. In: Jacobs W Jr, Hatfull G, eds. Molecular genetics of *Mycobacteria.* Washington, DC: ASM Press, **2000**:316–7.
13. Karakousis PC, Yoshimatsu T, Lamichhane G, et al. Dormancy phenotype displayed by extracellular *Mycobacterium tuberculosis* within artificial granulomas in mice. J Exp Med **2004**; 200:647–57.
14. Cole ST. TubercuList. WWW server v3.1. Available at: http://genolist.pasteur.fr/TubercuList/. Accessed 1 November 2006.
15. The Institute for Genomic Research. *Mycobacterium tuberculosis* CDC1551 genome. Available at: http://cmr.tigr.org/tigr-scripts/CMR/GenomePage.cgi?org_search=&org=gmt. Accessed 1 November 2006.
16. Kaushal D, Schroeder BG, Tyagi S, et al. Reduced immunopathology and mortality despite tissue persistence in a *Mycobacterium tuberculosis* mutant lacking alternative sigma factor, *SigH.* Proc Natl Acad Sci USA **2002**; 99:8330–5.
17. Karls RK, Guarner J, McMurray DN, Birkness KA, Quinn FD. Examination of *Mycobacterium tuberculosis* sigma factor mutants using low-dose aerosol infection of guinea pigs suggests a role for *SigC* in pathogenesis. Microbiology **2006**; 152:1591–600.
18. Sun R, Converse PJ, Ko C, Tyagi S, Morrison NE, Bishai WR. *Mycobacterium tuberculosis* ECF sigma factor *sigC* is required for lethality in mice and for the conditional expression of a defined gene set. Mol Microbiol **2004**; 52:25–38.
19. Bishai WR, Dannenberg AM Jr, Parrish N, et al. Virulence of *Mycobacterium tuberculosis* CDC1551 and H37Rv in rabbits evaluated by Lurie's pulmonary tubercle count method. Infect Immun **1999**; 67: 4931–4.
20. Murphy HN, Stewart GR, Mischenko VV, et al. The OtsAB pathway is essential for trehalose biosynthesis in *Mycobacterium tuberculosis.* J Biol Chem **2005**; 280:14524–9.
21. Betts JC, Lukey PT, Robb LC, McAdam RA, Duncan K. Evaluation of a nutrient starvation model of *Mycobacterium tuberculosis* persistence by gene and protein expression profiling. Mol Microbiol **2002**; 43:717–31.
22. Schnappinger D, Ehrt S, Voskuil MI, et al. Transcriptional adaptation of *Mycobacterium tuberculosis* within macrophages: insights into the phagosomal environment. J Exp Med **2003**; 198:693–704.
23. Manganelli R, Voskuil MI, Schoolnik GK, Dubnau E, Gomez M, Smith I. Role of the extracytoplasmic-function sigma factor sigma(H) in *Mycobacterium tuberculosis* global gene expression. Mol Microbiol **2002**; 45:365–74.
24. Muttucumaru DG, Roberts G, Hinds J, Stabler RA, Parish T. Gene expression profile of *Mycobacterium tuberculosis* in a non-replicating state. Tuberculosis (Edinb) **2004**; 84:239–46.
25. Sirakova TD, Dubey VS, Cynamon MH, Kolattukudy PE. Attenuation of *Mycobacterium tuberculosis* by disruption of a *mas*-like gene or a chalcone synthase-like gene, which causes deficiency in dimycocerosyl phthiocerol synthesis. J Bacteriol **2003**; 185:2999–3008.